

REAL-TIME MONITORING OF CREVICE CORROSION PROPAGATION RATES IN SIMULATED SEAWATER USING COUPLED MULTIELECTRODE ARRAY SENSORS

Xiaodong Sun and Lietai Yang
Corr Instruments, LLC
San Antonio, TX, USA

ABSTRACT

Real-time coupled multielectrode array sensor probes were used to measure the localized corrosion rates for Type 1008 carbon steel, Type 110 copper, and Type 316L stainless steel in simulated seawater under creviced and exposed conditions. The maximum localized corrosion rate, for the carbon steel probes measured under a crevice, was 10 to 25 times lower than that measured under exposed conditions; the localized corrosion inside the crevice was found to be in the form of pitting corrosion. The maximum localized corrosion rate for the stainless steel probes was similar to that measured without a crevice. The similarity of the localized corrosion behavior, with and without a crevice for the stainless steel probes, was attributed to the relatively large gap of crevice (0.089 mm) that was not tight enough to have a significant effect on the corrosion. An exposed large electrode, made from the same wire as that of the carbon steel probe electrodes, was placed near the probes and in the same solution, in order to simulate the metal surrounding a creviced area. The corrosion potential of the creviced probe was found to be higher than that of the exposed large metal electrode. When the creviced probe was coupled to the large metal electrodes in the simulated seawater, its corrosion rate decreased essentially to zero, and the sensing electrodes of the creviced probe were cathodically protected by the exposed large electrode.

Keywords: Corrosion monitoring, corrosion sensor, localized corrosion, online sensor, crevice corrosion, corrosion probe, crevice sensor, crevice probe, real-time sensor, multielectrode sensor, coupled multielectrode.

INTRODUCTION

Crevice corrosion is one of most common types of localized corrosion that cause metallic equipment and engineering structure failures.¹ The online and real-time measurements of crevice corrosion play an important role in corrosion control and mitigation. However, there are only a limited number of methods that can be used to quantitatively measure the propagation rate under crevices. Coupled multielectrode sensors (CMAS) have been recently used as *in situ* and online monitors for non-uniform corrosion, including localized corrosion—such as pitting corrosion—in cooling water pipes of

chemical plants²⁻³ and other laboratory and field systems.⁴⁻¹⁹ Some of the CMAS applications include quantitative and real-time localized corrosion monitoring for cathodically protected systems,¹⁰ coated metal components,^{11,16} metals in concrete,¹² metals in soil,¹⁵ and metals in low conductivity waters.¹⁸ In the present work, coupled multielectrode corrosion probes were used as an online tool for measuring the propagation rates in simulated seawater for Type 316L stainless steel (UNS S31603), Type 110 copper (UNS C11000), and Type 1008 carbon steel (UNS G10080). The measurements of localized corrosion rates under exposed conditions for these metals were also conducted, for comparison.

EXPERIMENTAL PROCEDURES

Coupled multielectrode sensors were used in the experiment. *Figure 1* shows the principle of a coupled multielectrode corrosion instrument,^{12,15} which couples the multiple sensing electrodes of the probe to a common joint through small resistors. Under a non-uniform corrosion condition (e.g., localized conditions), some of the electrodes corrode in preference to others and, therefore, dispersion in the measured currents from the sensing electrodes can be observed. Thus, the multiple electrodes in the probe simulate a single piece of metal.⁵⁻⁶ If the sensing elements are sufficiently small, so that separation of anodic and cathodic reactions between the different electrodes can be assumed, the maximum localized corrosion rates can be obtained directly from the measured current densities from these electrodes:

$$CR_{\max} = (1/\epsilon)I_{\max}^a W_e / (F\rho A) \quad (1)$$

Where CR_{\max} is the calculated maximum penetration rate (cm/s), ϵ is the current distribution factor (fraction of the electrons produced on the most corroding electrode that flows to the other electrodes through the coupling circuit), F is the Faraday constant (96485 C/mol), A is the surface area of the electrode (cm²), ρ is the density of the alloy or electrode (g/cm³), and W_e is the equivalent weight (g/mol). Under conditions where localized corrosion is significant, the most corroding electrode is usually significantly different from the other electrodes, and, therefore, the current distribution factor, ϵ , is usually close to unity. The I_{\max}^a in Equation (1) is simply the highest anodic current directly measured from the coupled multielectrode array sensor probe.

Accordingly, the maximum penetration depth (cm) may be calculated by:

$$H_{\max} = (1/\epsilon)Q_{\max}^a W_e / (F\rho A) \quad (2)$$

Where Q_{\max}^a is the maximum of the cumulative anodic charges (coulomb) from all the electrodes. It should be noted that I_{\max}^a and Q_{\max}^a may or may not be from the same electrodes.

The coupled multielectrode instrument used in the experiment was a nanoCorr¹ Model S-50 coupled multielectrode analyzer,²⁰ manufactured by Corr Instruments (San Antonio, TX, USA) (*Figure 2*). This CMAS corrosion analyzer has a current resolution below 10⁻¹² A and allows the measurement of coupling currents for up to 50 electrodes. With the factory supplied CorrVisual¹ software, this analyzer simultaneously measures the real-time maximum localized corrosion rates and maximum localized penetration depth, average corrosion rates and average penetration depth, corrosion potentials, temperature and other parameters from: four independent coupled multielectrode probes, three pH or

¹ nanoCorr and CorrVisual are trademarks of Corr Instruments, LLC

three oxidation/reduction potential (ORP) probes, or three other transducers for parameters, such as conductivity, humidity, flow, and pressure.

Figure 3 shows typical CMAS probes used to obtain the data under both creviced and un-creviced conditions. In a typical un-creviced probe, the sensing miniature electrodes were flush-mounted in epoxy and polished to 400 or 600 grits before use. In a creviced probe, one or more layers of acid-free paper (0.5 by 0.5 inch [1.27 by 1.27 cm] in square and 0.0035 inch [0.089 mm] in thickness per layer) were fixed onto the pre-polished sensing surface of the probe by placing a disk-shaped epoxy paste on the top. Two sides of the disk, after it was cured, were cut so that the edges of the paper under the epoxy could be exposed. During the experiment, the electrolyte soaked the paper. The wetted space (the paper thickness) formed the crevice. The tightness of the crevice was controlled by selecting the proper thickness of the paper or the proper number of layers of the paper. Alternatively, the paper can be replaced by a layer of Polytetrafluoroethylene (PTFE) to form an even tighter crevice. The electrodes on the three creviced probes shown in *Figure 3* were made of 1 mm-diameter wires. The equivalent weight values given to the software for the calculation of corrosion rate and corrosion depth were 25.5, 63.55, and 27.9 for the Type 316L stainless steel (SS316L), Type 110 copper (CDA110), and Type 1008 carbon steel (CS1008), respectively.

The experiment was conducted in a beaker filled with simulated seawater that contained 3%wt sea salt by Vigo Importing Co. (Tampa, Florida, USA). The CMAS probes, temperature probe, pH probe, and ORP probe were vertically immersed in the simulated seawater, which was not agitated during the experiments. A silver/silver chloride (Ag/AgCl) electrode was used as the reference electrode for the electrochemical potentials of the probes and ORP. The experiment was conducted at a temperature range from 21 to 27° C.

Under crevice corrosion conditions, the creviced area is usually the anodic area and the metal outside the creviced area usually serves as the cathode. Two wire loops—one made of the CS1008 wire used for the CS1008 probe and the other made of CDA110 wire used for the CDA100 probe—were immersed in the solution near their respective creviced probes, to act as the metals outside of the crevices. The ratio of the exposed surface area of the CS1008 loop to the surface area of the CS1008 probe sensing electrodes was 76.8; the ratio of the exposed surface area of the CDA110 loop to the surface area of the CDA110 probe sensing electrodes was 57.5.

A notebook computer was used to collect the data from the multielectrode analyzer. The current from each electrode, the electrochemical potential (the coupling potential) of each probe, and the temperature were logged at a predetermined interval (usually 20 to 600 seconds) and saved in a computer file. Processed signals (such as the maximum localized corrosion current, the maximum cumulative charge, the average corrosion rate and the average cumulative corrosion damage or penetration depth) for each probe were also saved in one or more separate data files. During the measurements, all the directly measured currents and the processed results (such as the minimum current, maximum current, mean current, current densities, maximum localized corrosion rates, average corrosion rate, cumulative charges, maximum localized corrosion penetration depth, average corrosion depth, and electrochemical potential) were dynamically displayed from the computer screen in both numerical and graphical forms. The configuration parameters for data acquisition were also available on the computer screen and most of them could be changed any time (dynamically) during the test.

RESULTS AND DISCUSSIONS

Localized Corrosion Rates and Other Signals from Creviced Probes

Figure 4 shows the measured maximum localized corrosion rates from the crevice CS1008, CDA110, SS316L CMAS probes. The maximum localized corrosion rate from the CS1008 probe was relatively high initially (~200 $\mu\text{m}/\text{yr}$ or 8 mil/yr) in the first week of testing, and stabilized at approximately 100 $\mu\text{m}/\text{yr}$ (4 mil/yr) during the remaining four weeks of testing. The maximum localized corrosion rate averaged over the entire testing period for the CS1008 probe was 126 $\mu\text{m}/\text{yr}$ (5 mil/yr). The maximum localized corrosion rate from the CDA110 probe was approximately 16 $\mu\text{m}/\text{yr}$ (0.63 mil/yr) initially and fluctuated between 20 $\mu\text{m}/\text{yr}$ (0.79 mil/yr) and 71 $\mu\text{m}/\text{yr}$ (2.8 mil/yr). The maximum localized corrosion rate averaged over the entire testing period for the CDA110 probe was 32 $\mu\text{m}/\text{yr}$ (1.3 mil/yr). The maximum localized corrosion rate from the SS316L probe was from 0.1 to 0.15 $\mu\text{m}/\text{yr}$ (0.004 to 0.006 mil/yr) most of the time, except on two occasions when the maximum rate increased to 0.6 $\mu\text{m}/\text{yr}$ (0.024 mil/yr) and 1.7 $\mu\text{m}/\text{yr}$ (0.067 mil/yr). The two localized corrosion rate peaks from the SS316L probe indicated two instances of initiation of localized corrosion and passivation on the Type 316L metal in the simulated seawater. The maximum localized corrosion rate, averaged over the entire testing period for the SS316L probe, was 0.19 $\mu\text{m}/\text{yr}$ (0.0075 mil/yr).

Figure 5 shows the corrosion potentials for the three creviced probes. The corrosion potential of the creviced carbon steel probe was from -0.680 to -0.643 V(Ag/AgCl) in the first four weeks and it increased to -0.578 V(Ag/AgCl) by the end of the five-week testing. The corrosion potential of the creviced CDA110 probe varied between -0.031 V(Ag/AgCl) and -0.219 V(Ag/AgCl). The corrosion potential of the creviced stainless steel probe increased steadily from -0.114 V(Ag/AgCl) at the beginning to 0.119 V(Ag/AgCl) by the end, except for two valleys that corresponded to the two maximum localized corrosion rate peaks as shown in *Figure 4*. These two valleys indicate that the probe was active during the initiation and propagation of localized corrosion on the probe.

Figures 6 and 7 show the ORP, pH and temperature during the testing period. The pH was approximately 7 throughout the test. The ORP was near 0.250 V(Ag/AgCl) during the first three weeks of testing, but peaked to 0.350 V(Ag/AgCl) in the fourth week and was relatively high in the fifth week. It is not known what caused the increase in the ORP; the solution was not agitated. The temperature was nearly constant (27 °C) during the entire testing period, except in the last day when the temperature started to decrease and reached 23 °C at the end.

Figure 8 shows the creviced CS1008 probe after the 35-day testing in simulated seawater. Pitting was apparent on most of the electrode surfaces after the corrosion products were removed, which is consistent with the observed relatively high maximum localized corrosion rates (average localized rate: 126 $\mu\text{m}/\text{yr}$, see *Figure 4*).

Figure 9 shows the creviced SS316L probe after the 35-day testing in simulated seawater. Rust was only found on Electrode #1. After removal of the small amount of rust on the probe's sensing surface, all electrodes of the probe looked intact; the polishing marks were clearly visible on all electrodes, which is consistent with the observed relatively low average localized corrosion rate (0.19 $\mu\text{m}/\text{yr}$, see *Figure 4*). The localized corrosion sign for Electrode #1 (the rust on Electrode #1) is consistent with the currents shown in *Figure 10*, which shows that only Electrode #1 was anodic during the period that the high maximum localized corrosion rate was measured.

Comparison with the Localized Corrosion Rates from Un-creviced Probes

Figure 11 shows the comparison for the maximum localized corrosion rates in simulated seawater obtained from the same CS1008 probe before and after the crevice was formed. The maximum localized corrosion rate from the un-creviced probe was approximately 10 to 25 times higher than that from the creviced probe. This is consistent with the hypothesis by Cottis²¹ and later observed by Roberge^{22, 23} that carbon steel corrodes less under creviced areas than in the exposed areas in seawater. It was not expected that the acid-free paper used in the crevice would be an inhibitor for corrosion. The lower localized corrosion rate under the crevice was probably due to the reduced degree of mass transfer for the corrosion reactants and the products inside the crevice.

Figures 12 and 13 show the comparisons for the maximum localized corrosion rates in simulated seawater obtained with and without crevice from the same SS316L and CDA110 probes, respectively. For these two metals, there was no significant difference between the corrosion rates with crevice and the corrosion rate without crevice. This is probably due to the fact that the corrosion rate on the exposed metal surface for these two types of metals is already low enough and the limit on mass transfer by the crevice did not produce a significant difference. In addition, the crevice formed by one layer of the paper (0.089 mm thick) was probably too large for these metals. If a PTFE tape had been used, instead of the paper that soaks electrolytes, the results might have been different.

Corrosion Potentials and Corrosion Rates of Creviced Probes Before and After Coupling to Exposed Large Electrodes

Figure 14 shows the potentials of the creviced CS1008 and the creviced CDA110 probes, the potentials of the exposed large CS1008 and large CDA100 metals, and the potentials of the two probes after they were coupled to their respective exposed large electrodes. For both of the metals, the corrosion potentials of the creviced probes were consistently higher than those of their exposed large counterpart metals. After the creviced probes were coupled to their respective exposed large metals, the potential of the exposed large metal remained essentially unchanged and the potentials of the probes were equal to the potentials of their corresponding exposed electrodes. Because the potentials of the two probes were lowered by their corresponding exposed large electrodes, the electrodes in the probes were cathodically protected. This is reflected in the maximum localized corrosion rates measured from the two probes (*Figure 15*). The maximum localized corrosion rates from the two creviced probes became essentially zero, as soon as the probes were coupled to their corresponding exposed large electrodes. This is consistent with the discussion by Cottis that carbon steel is not subject to crevice corrosion in seawater, because the exposed surface is highly active and there is no cathodic site on the exposed surface to support the crevice corrosion.²¹

CONCLUSION

Real-time coupled multielectrode array sensor probes were used to measure the maximum localized corrosion rates with and without crevices for Type 1008 carbon steel, Type 110 copper, and Type 316L stainless steel in simulated seawater. For the carbon steel probe, the maximum localized corrosion rate measured without the crevice was 10 to 25 times higher than that with the crevice (0.089 mm crevice gap). The localized corrosion inside the crevice was found to be in the form of pitting corrosion. For the copper and stainless steel probes, the maximum localized corrosion rates were found to be similar to their respective values with and without the crevices. It was considered that the crevice (0.089 mm gap) was not tight enough for these two metals.

Exposed large carbon steel and copper electrodes, which were made of the same wires as those of the electrodes in the creviced carbon steel and copper probes, were placed near their respective probes in the same solution, to simulate the metals surrounding creviced areas. For both the carbon steel and the copper, the corrosion potentials of the creviced probe were found to be higher than those of their corresponding exposed large metal electrodes. When the probes were coupled to their respective large metal electrodes in the simulated seawater, the corrosion rates of the probes decreased essentially to zero, suggesting that the sensing electrodes under the crevices were cathodically protected by the exposed large metal surrounding the crevices.

REFERENCES

1. G.S. Frankel, and J.R. Scully, Ed, "Localized Corrosion, Proceedings of the Corrosion/2001 Research Topical Symposium," NACE International, 2001.
2. M. H. Dorsey, L. Yang and N. Sridhar, "Cooling Water Monitoring Using Coupled Multielectrode Array Sensors and Other On-line Tools," CORROSION/2004, paper no. 04077, (Houston, TX: NACE International, 2004).
3. Michael H. Dorsey, Daniel R. Demarco, Brian J. Saldanha, George A. Fisher, Lietai Yang and Narasi Sridhar, "Laboratory Evaluation of a Multi-Array Sensor for Detection of Underdeposit Corrosion and/or Microbially Influenced Corrosion," CORROSION/2005, paper no. 05371 (Houston, TX: NACE, 2005).
4. L. Yang and N. Sridhar, "Monitoring of Localized Corrosion ASM Handbook," Volume 13A-Corrosion: Fundamentals, Testing, and Protection, Stephen. D. Crammer and Bernard S. Covino, Jr., Eds., ASM International, Materials Park, Ohio, 2003, pp 519-524.
5. L. Yang, N. Sridhar, O. Pensado, and D.S. Dunn, *Corrosion*, 58 (2002), p.1004.
6. L. Yang and N. Sridhar, "Coupled Multielectrode Online Corrosion Sensor," *Materials Performance*, 42 (9), pp 48-52 (2003).
7. L. Yang, R.T. Pabalan, L. Browning, and G.C. Cragolino, "Measurement of Corrosion in Saturated Solutions under Salt Deposits Using Coupled Multielectrode Array Sensors," CORROSION/2003, paper no. 426 (Houston, TX: NACE, 2003).
8. L. Yang, R. T. Pabalan, L. Browning and D.S. Dunn, "Corrosion Behavior of Carbon Steel and Stainless Steel Materials under Salt Deposits in Simulated Dry Repository Environments," in *Scientific Basis for Nuclear Waste Management XXVI* R. J. Finch and D. B. Bullen, Eds., Warrendale, PA: Materials Research Society, M.R.S. Symposium Proceedings Vol. 757, pp.791-797, 2003.
9. C.S. Brossia and L. Yang, "Studies of Microbiologically Induced Corrosion Using a Coupled Multielectrode Array Sensor," CORROSION/2003, paper no. 575 (Houston, TX: NACE, 2003).
10. X. Sun, Xiaodong Sun, "Online Monitoring of Corrosion under Cathodic Protection Conditions Utilizing Coupled Multielectrode Sensors," CORROSION/2004, paper no. 04094, (Houston, TX: NACE International, 2004).

11. X. Sun, "Online Monitoring of Undercoating Corrosions Utilizing Coupled Multielectrode Sensors," CORROSION/2004, paper no.04033 (Houston, TX: NACE, 2004).
12. X. Sun, "Online and Real-Time Monitoring of Carbon Steel Corrosion in Concrete, Using Coupled Multielectrode Sensors," CORROSION/2005, paper no.05267 (Houston, TX: NACE, 2005).
13. Lietai Yang, Darrell Dun and Gustavo Cragnolino, "An Improved Method for Real-time and Online Corrosion Monitoring Using Coupled Multielectrode Array Sensors," CORROSION/2005, paper no. 05379, (Houston, TX: NACE International, 2005).
14. Lietai Yang, Darrell Dun, Yi-Ming Pan and Narasi Sridhar, "Real-time Monitoring of Carbon Steel Corrosion in Crude Oil and Salt Water Mixtures Using Coupled Multielectrode Sensors," CORROSION/2005, paper no. 05293, (Houston, TX: NACE International, 2005).
15. Xiaodong Sun, "Real-Time Corrosion Monitoring in Soil with Coupled Multielectrode Sensors." CORROSION/2005, paper no.05381 (Houston, TX: NACE, 2005).
16. Xiaodong Sun, "Online Monitoring of Undercoating Corrosion Using Coupled Multielectrode Sensors," Materials Performance, 44 (2), p28-32 (2005).
17. A. Anderko, N. Sridhar¹ and L. Yang, S.L. Grise, B.J. Saldanha, and M.H. Dorsey, "Validation of a Localized Corrosion Model Using Real-Time Corrosion Monitoring in a Chemical Plant," Corrosion Engineering, Science and Technology (formerly British corrosion J.), Vol. 40, pp.33-42, August (2005).
18. X. Sun and Lietai Yang, "Real-Time Monitoring of Localized Corrosion in Drinking Water Utilizing Coupled Multielectrode Array Sensors," CORROSION/2006, paper no. 06094, (Houston, TX: NACE International, 2006).
19. Xiaodong Sun and Lietai Yang, "Real-Time Monitoring of Localized and General Corrosion Rates in Simulated Marine Environments Using Coupled Multielectrode Array Sensors," CORROSION/2006, paper no.06284 (Houston, TX: NACE, 2006).
20. Corr Instruments, "nanoCorr S-50 Multielectrode Analyzer for Real-Time Monitoring of Corrosion Rate, pH, ORP and Others," Materials Performance, 44 (3), p100 (2005).
21. R. Cottis, "Crevice Corrosion of Steel in Seawater", E-mail to NACE Internal Network, August 17, 2004.
22. P. R. Roberge, "Crevice Corrosion of Steel in Seawater", E-mail to NACE International Network, September 20, 2004.
23. P.R. Roberge, "Crevice Susceptibility", <http://corrosion-doctors.org/Experiments/crevice-g78-test.htm>, October, 2004.

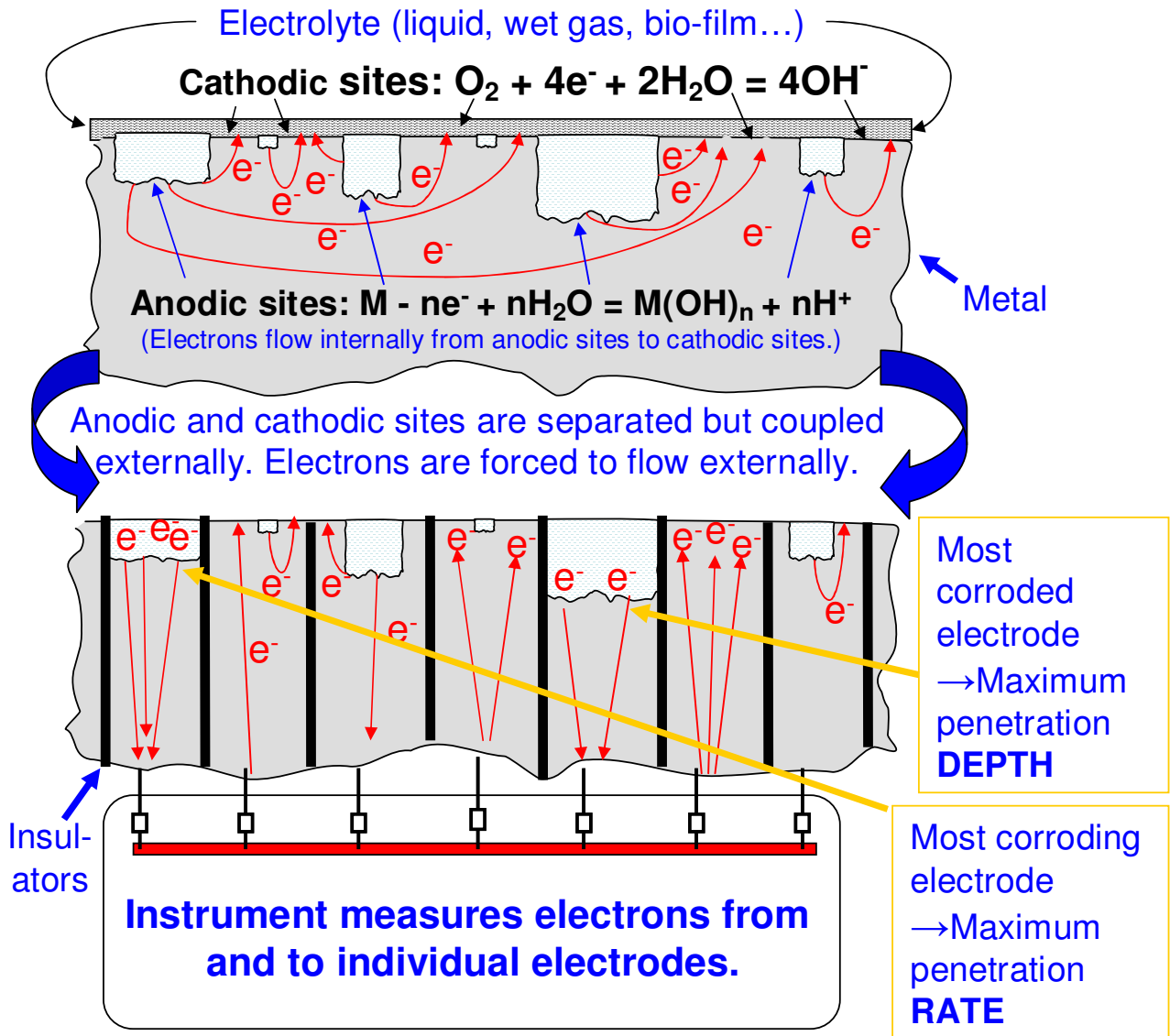


Figure 1. Schematic diagram showing the principle of the coupled multi-electrode array sensor analyzer for the measurement of localized corrosion.¹⁵ The maximum localized corrosion rate from the instrument represents the penetration rate of the most corroding electrode (e.g., 1st electrode from the left in the bottom figure). The maximum localized penetration depth from the instrument represents the corroded depth of the most corroded electrode (e.g., 5th electrode from the left in the bottom figure). The general or average corrosion rate is calculated from the average of the anodic currents, and the general or average corrosion depth is calculated from the average of the anodic charges.



Figure 2. Coupled multi-electrode analyzer used in the experiments and typical real-time displays on a notebook computer (see insert).

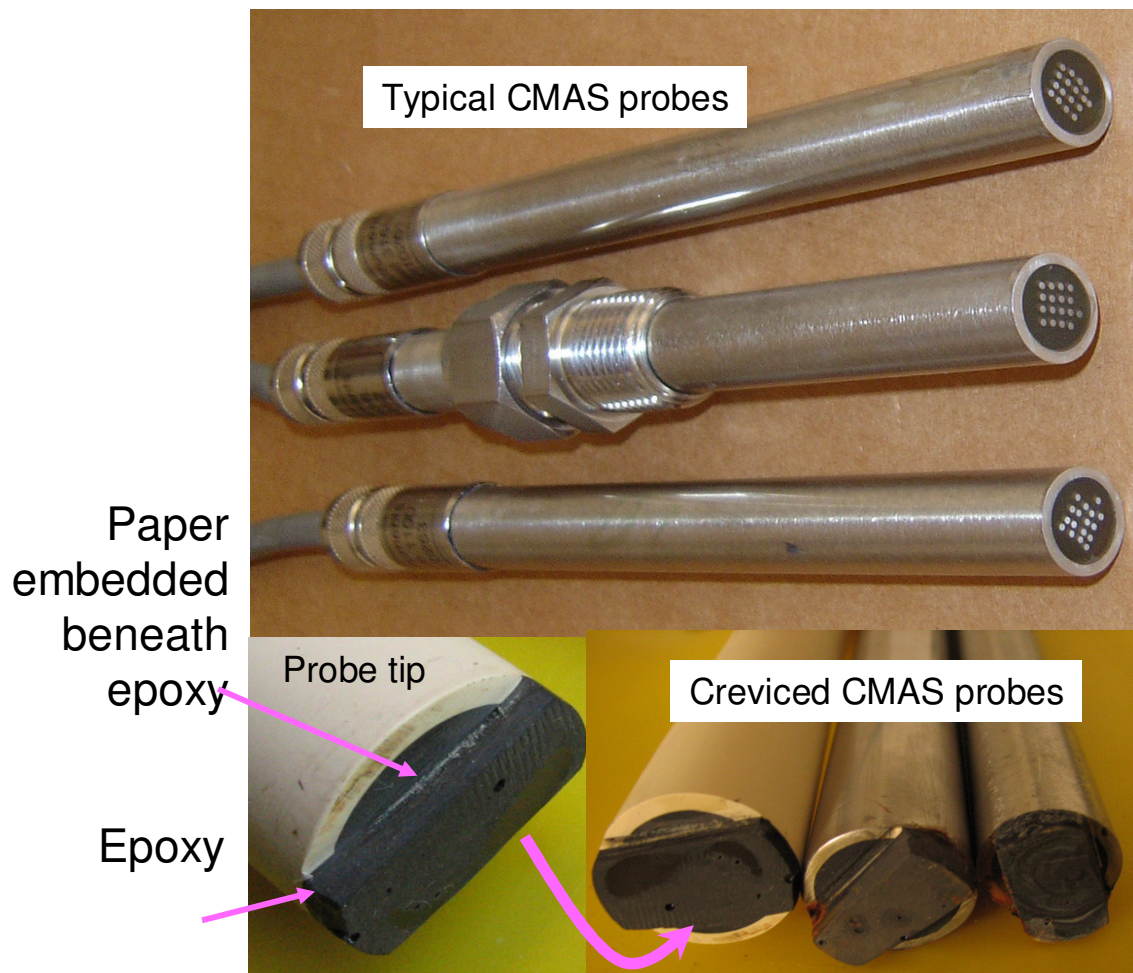


Figure 3. Typical coupled multielectrode array sensor (CMAS) probes and the creviced CMAS probes used in the experiments. The crevice was formed by imbedding a layer of acid-free paper between the sensing surface and epoxy; tightness of crevice is controlled by selecting the thickness of the paper or number of layers of the paper; the paper will be soaked with the testing solution during the experiment.

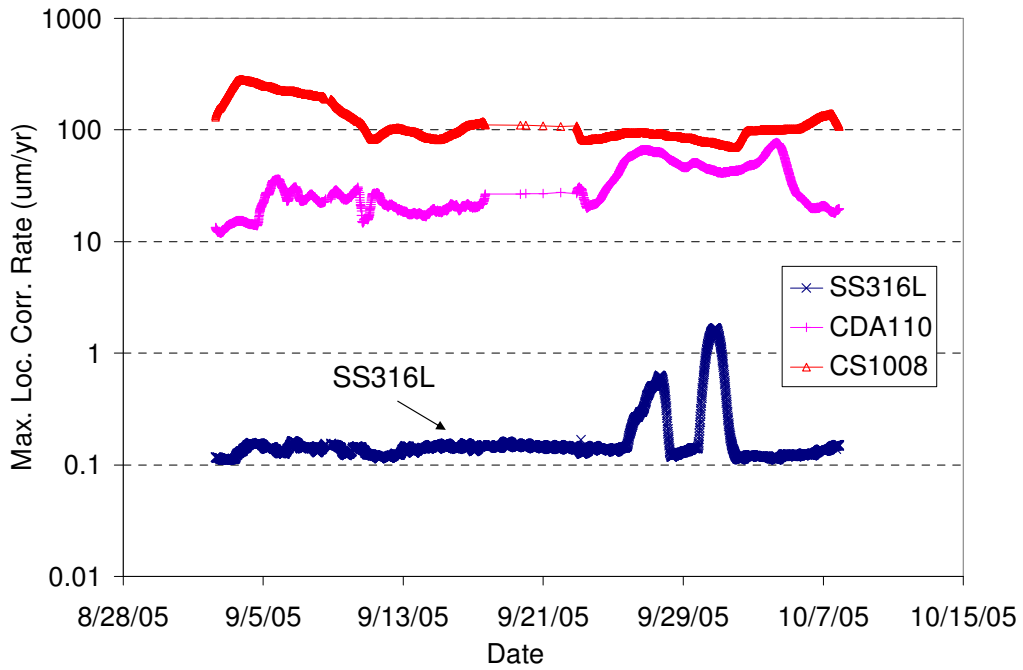


Figure 4. Maximum localized corrosion rate measured from three creviced CMAS probes in simulated seawater at room temperature. Note: um/yr means $\mu\text{m/yr}$.

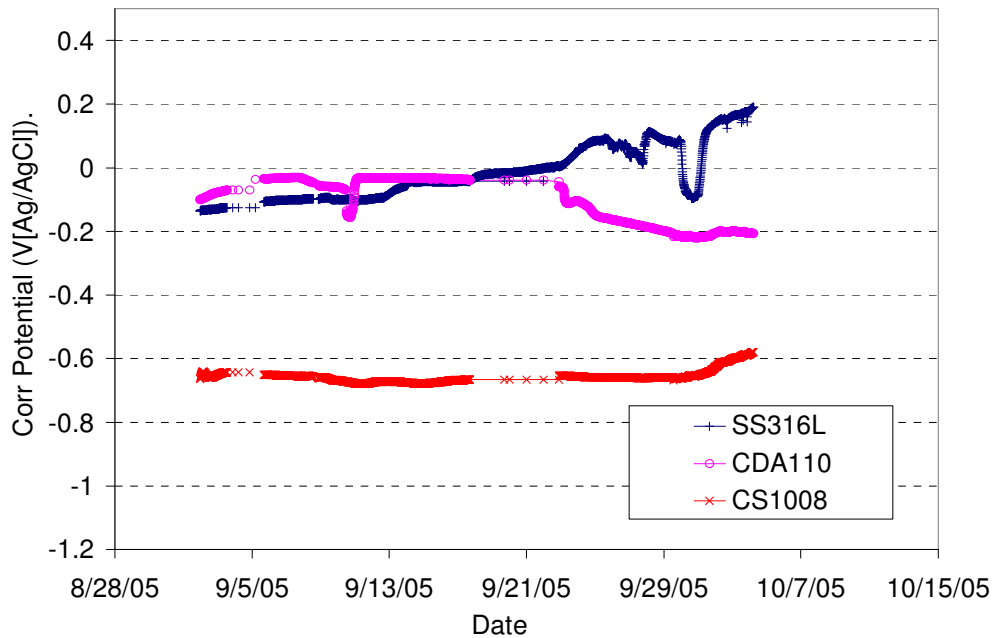


Figure 5. Corrosion potentials of the three CMAS probes during the test for the data as shown in *Figure 4*.

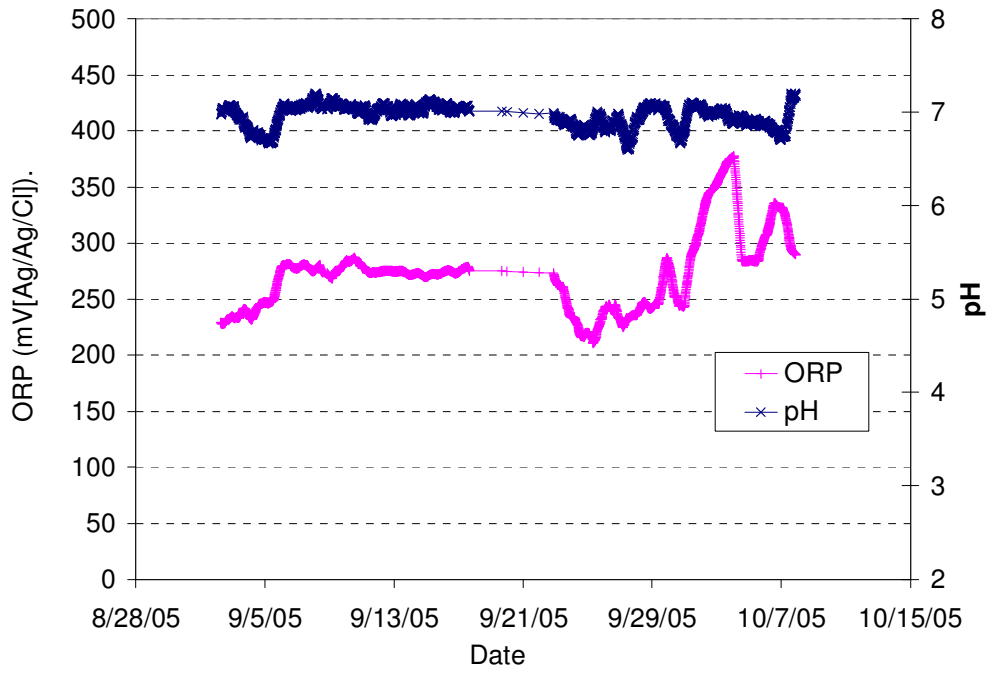


Figure 6. Oxidation/Reduction Potential (ORP) and pH of the simulated seawater during the test for the data as shown in *Figure 4*.

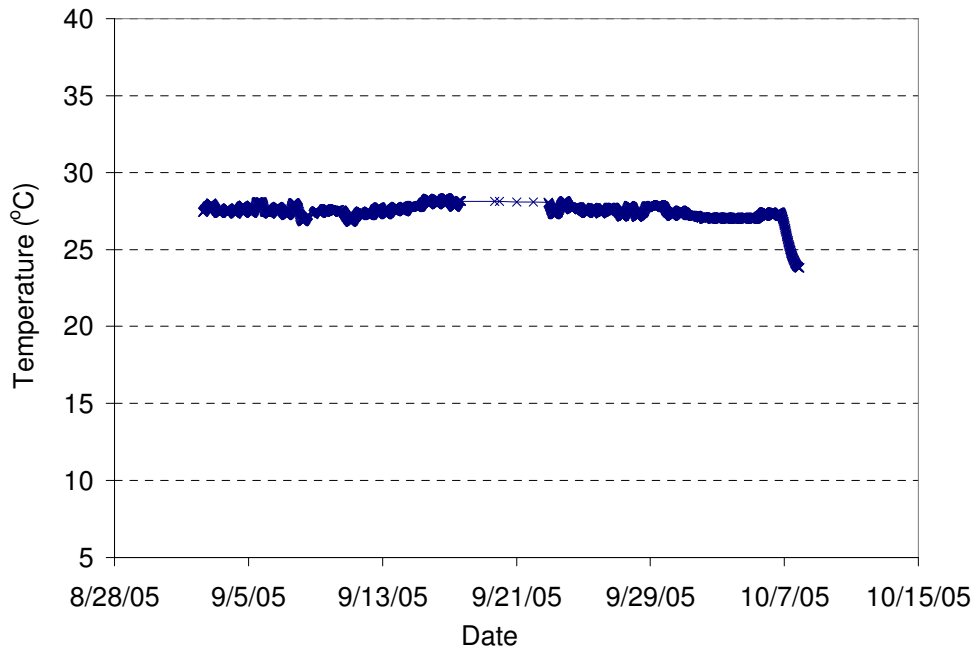


Figure 7. Temperature of the simulated seawater during the test for the data as shown in *Figure 4*.

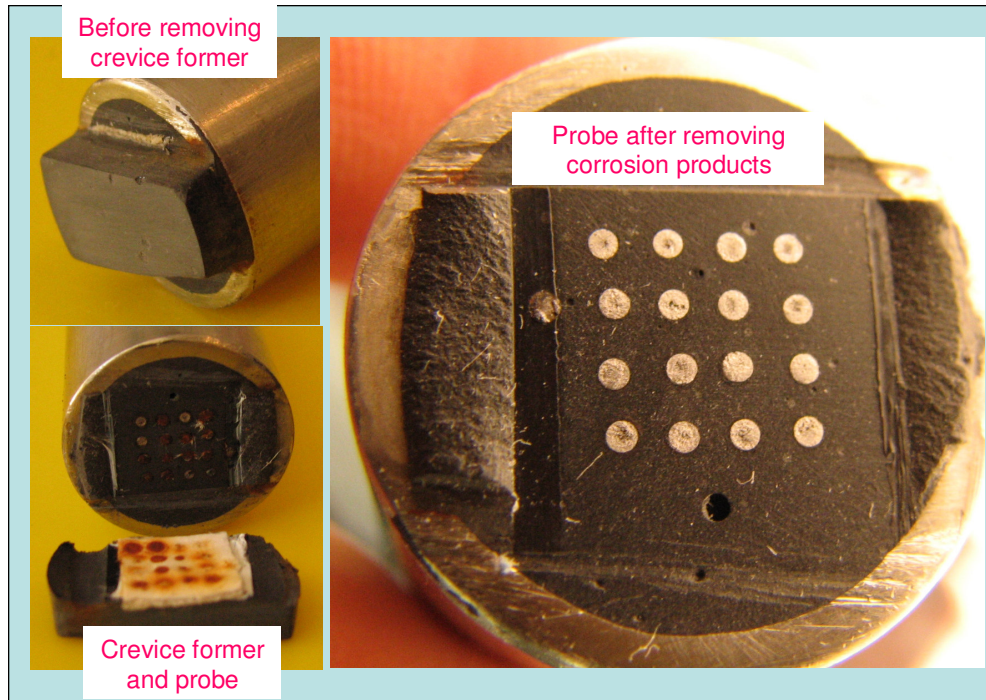


Figure 8. Creviced Type 1008 carbon steel CMAS probe after 35-day testing in simulated seawater. Pitting was apparent after the corrosion products were removed.

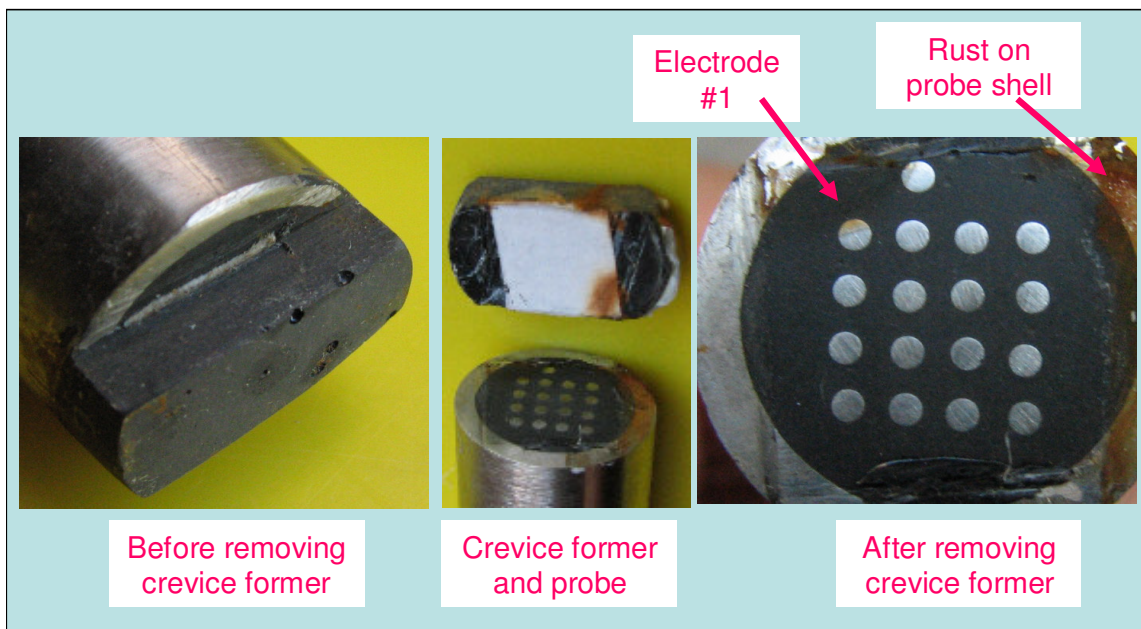


Figure 9. Creviced Type 316L stainless steel CMAS probe after 35-day testing in simulated seawater. Rust was found on Electrode #1 and one side of the probe shell made of Type 316L stainless steel. It was noticed that the epoxy crevice former disbonded from the probe shell at the location where rust was found.

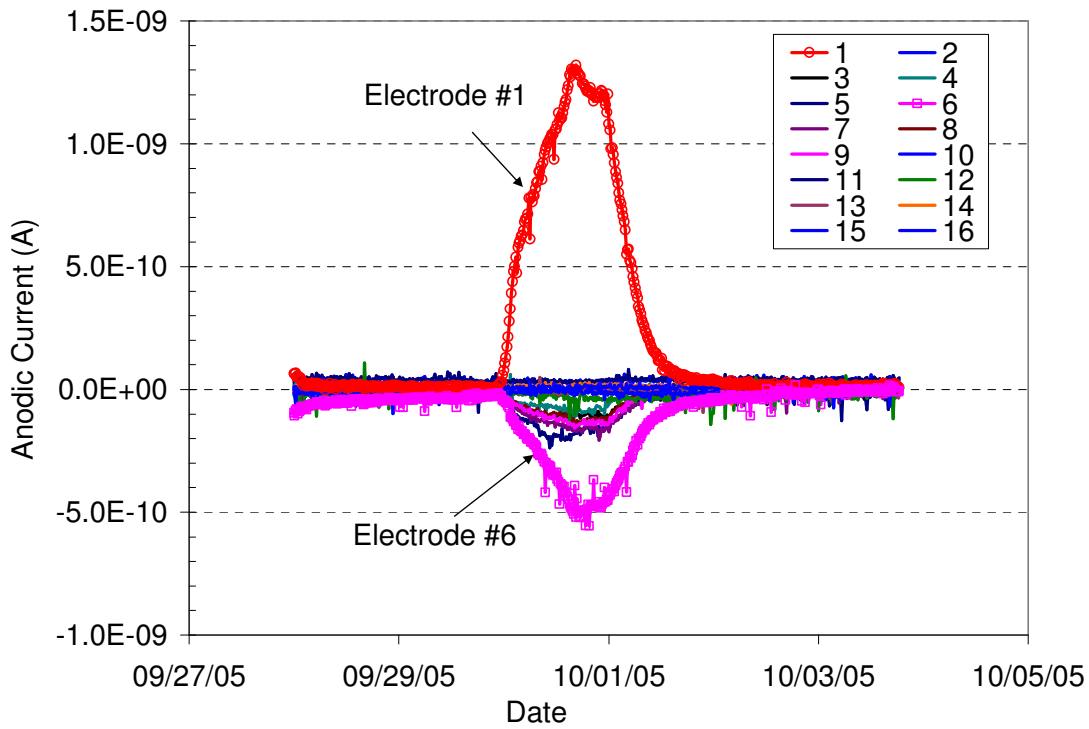


Figure 10. Currents from the 16 electrodes of the SS316L probe, when the maximum localized corrosion rate increased (see Figure 4). The observed corrosion rate was due to the anodic behavior of Electrode #1.

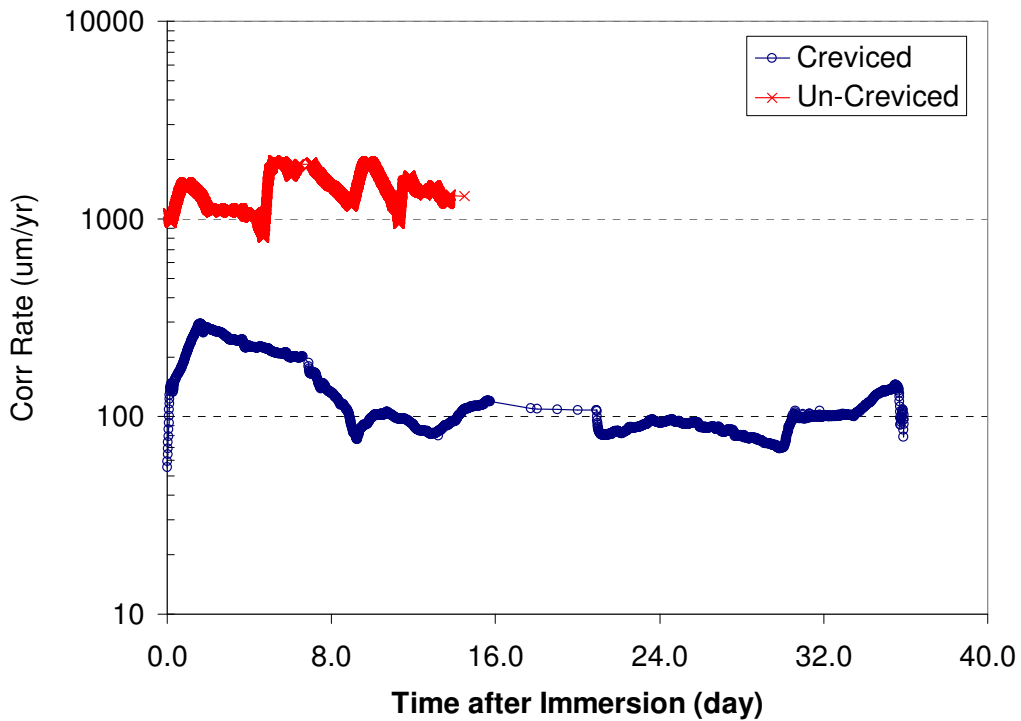


Figure 11. Comparison for the maximum localized corrosion rates obtained with and without crevice for the Type 1008 carbon steel CMAS probe in simulated seawater.

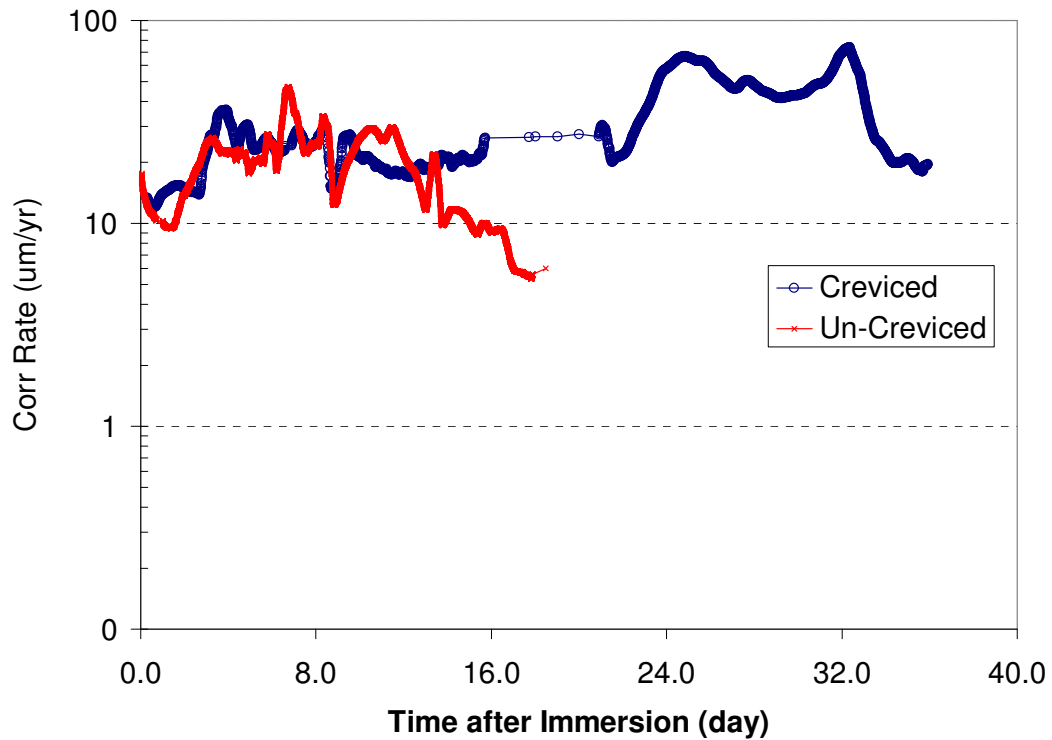


Figure 12. Comparison for the maximum localized corrosion rates obtained with and without crevice for the CDA110 copper CMAS probe in simulated seawater.

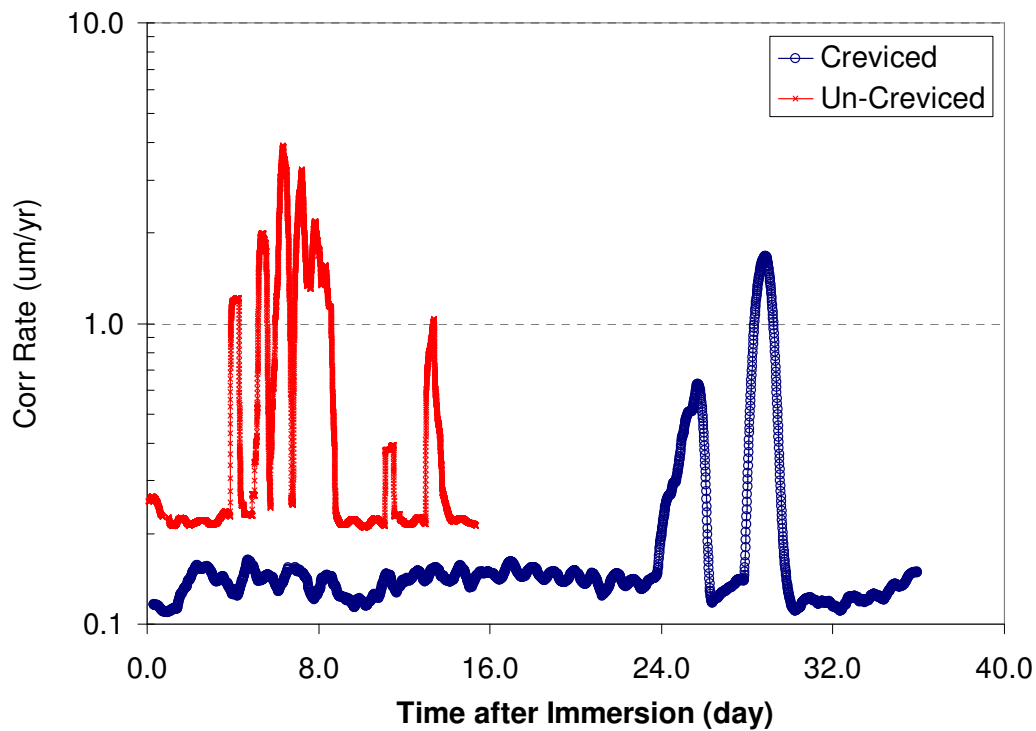


Figure 13. Comparison for the maximum localized corrosion rates obtained with and without crevice for the Type 316L stainless steel CMAS probe in simulated seawater.

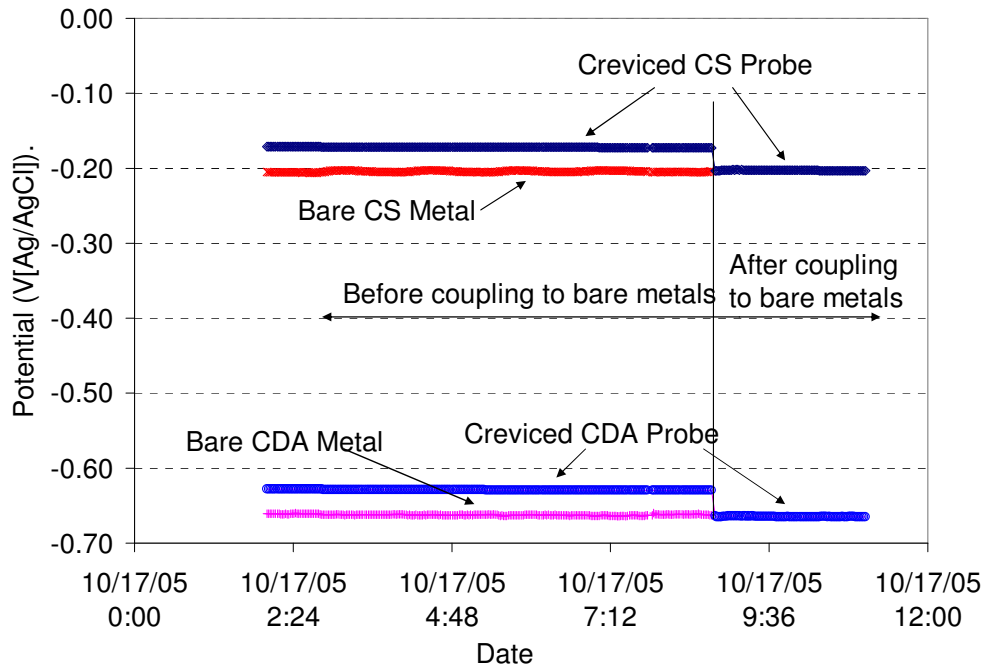


Figure 14. Corrosion potentials of the two creviced CMAS probes and two exposed large bare metal electrodes, and the potentials of the two probes after they were coupled to their respective bare metal electrodes. The potential of the creviced probes were lowered by their respective large bare metal electrodes.

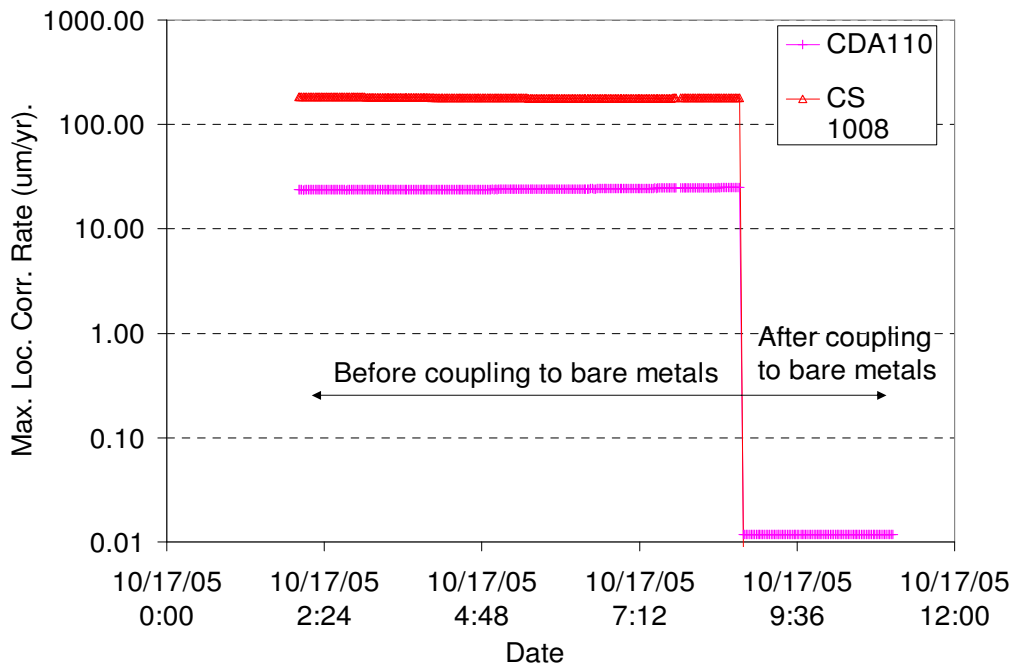


Figure 15. Maximum localized corrosion rates from the creviced CS 008 and CDA110 probes before and after they were coupled to their respective large bare metal electrodes. The electrodes in the creviced probes were cathodically protected after they were connected to their respective large bare metal electrodes.